

FWD: J1461

Sanda Kronberga <sanda-kro@inbox.lv>

Wed 12/27/2017 2:20 PM

To: Marina Romanova <Marina.Romanova@rtu.lv>;

----- Forwarded message -----

Subject: J1461

Date: Sat, 23 Dec 2017 19:06:44 0200

From: R.D.Adams@bristol.ac.uk

To: Sanda Kronberga ,

Dear Dr Kronberga

Thank you for sending me your paper. It has the reference **J1461**. Please always use this for correspondence.

I will send your paper out to referees and be in contact with you in due course

Yours sincerely

Bob Adams

*Professor Robert D. Adams, BSc[Eng], DSc[Eng] (London), PhD, ScD (Cambridge),*

*FIMechE, FInstP, ACGI, CEng,*

*Joint Editor in Chief, International Journal of Adhesion and Adhesives*

*Visiting Professor*

*Department of Engineering Science*

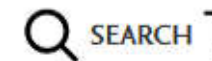
*University of Oxford*

*Emeritus Professor of Applied Mechanics*

*Department of Mechanical Engineering*



ELSEVIER



SEARCH

## Submission

Authors are requested to either submit their manuscript by e-mail or send by post their original manuscript and figures with three copies to one of the following Editors. If your document is larger than 5MB, please submit via post.

### Joint Editors-in-Chief:

Professor R. D. Adams (Mechanics, Engineering and Applications Papers),  
Department of Engineering Science, University of Oxford, Parks Road, Oxford,  
OX1 3PJ, UK; ✉ [R.D.Adams@bristol.ac.uk](mailto:R.D.Adams@bristol.ac.uk)

Professor Steve (S.J.) Shaw (Chemistry and Physics papers), Defence Science and  
Technology Laboratory, Porton Down, Salisbury, SP4 0JQ, UK; ✉  
[sjshaw26@hotmail.co.uk](mailto:sjshaw26@hotmail.co.uk)

The Journal welcomes scientifically robust research and reviews related to the dental adhesion theme. To submit your work, or for more information please contact:

### Subject Editor in Dental Adhesion

Dr. William Palin, The School of Dentistry, College of Medical and Dental

# Towards polymer composite reinforced by electrically charged nanoparticles

Yuri Dekhtyar, Sanda Kronberga\*, Marina Romanova,

Riga Technical University, Institute of Biomedical Engineering and Nanotechnologies 1 Kalku street,  
Riga LV1658, Latvia

\* *Person for communication, email: sanda-kro@inbox.lv*

Key words: epoxides, composites, nanoparticles, surface treatment, fracture, non-destructive testing, elastic modulus

## ABSTRACT

Strength and elastic modulus of the polymer composite material embedded with electrically charged silica nanoparticles were engineered. For this the electrical charge was deposited onto the nanoparticle surface because of ultraviolet radiation. The specimens were tested under mechanical loading (stretch), and their surface destruction was indicated *in situ* due to measurements of the emission of electrons.

The electrically charged nanoparticles embedded into the polymer composite material are able to control its strength and elastic module in dependence on the ultraviolet radiation exposure. The early destruction of the surface identified by electron emission appears at  $\sim 0.018$  of relative elongation.

## 1. INTRODUCTION

Nanoparticles (NP) are in use to reinforce polymer composites (PC) and control their mechanical properties. To reach this an adhesion of the NP surface to the polymer binder should be provided. In such a case the NP surface is functionalized, for instance, because of the specific coating deposition that supplies chemical coupling of the NP to the binder. [1]

Following the general adhesion theory [2] the attractive and repulsion forces compete to connect the particle surface to the binder. Because the repulsion employs the electrical fields [2] NP having an electrical charge arranged at their surface could be engaged to design the reinforced polymer composite and control its mechanical properties. The present article experimentally explores such the possibility for the first time.

## 2. EXPERIMENTAL PROCEDURE

The experiment was supplied in the following steps:

- deposition of the electrical charge onto the NP surface,
- preparation of the polymer composite specimens embedded with the electrically functionalized NP (FNP),
- stretch test of the specimens to identify the influence of the FNP on the PC mechanical properties,
- identification of the specimens early destruction *in situ* of stretching.

### 2.1. Deposition of the electrical charge onto the NP surface

The SiO<sub>2</sub> dielectric NP (Sigma Aldrich, reference number 637238, diameter 10-20 nm, density 2,2-2,6 g/ml at 25°C temperature) were in use for the experiment. The electrical charge deposition on the NP surface was reached because of the NP radiation by the ultraviolet light (UV) aimed to excite the SiO<sub>2</sub> electrons/holes from the valance band or/and local levels/bands and to be trapped by the local states situated at the surface [3]. The UV was supplied from the Hamamatsu Photonics source Lightningcure LC5 equipped with the Hamamatsu L8251 mercury Mercury-Xenon (200W) that delivered the UV in a range of 220-700 nm. The NP powder was located at the distance 30 cm from the UV source and was exposed with the light flow 3,89 W/cm<sup>2</sup> (at 365 nm wave length in accordance with the Lightningcure LC5 technical specification [4]). The specimens were exposed in a range from 0 to 60 minutes at the room condition.

The electrical charge deposited onto the NP surface was identified because of the electron work function (the potential barrier for the electron to escape, that directly connected to the surface electrical charge density) measurements [5]. An alteration of the electron work function ( $\phi$ ) induced by UV exposure was measured. To quantify the magnitude of  $\phi$  the photoelectron emission (PE) current (I) spectra of the NP powder were measured in accordance with the general photoemission formula:

$$I \sim (h\nu - \phi)^m ,$$

$h\nu$  – energy of the photons that excite photoemission,  
 $m$  – power index, could be acquired from the experiment.

The value of  $\phi$  was identified for the condition  $I=0$ , i.e.  $\phi=h\nu$ .

The handmade spectrometer [6] was employed to reach measurements of  $I(h\nu)$ . The PE was induced in a vacuum condition  $10^{-3}$  Pa. The values of  $\phi$  were achieved with the uncertainty  $<0.04$  eV. The Figure 1 demonstrates  $\phi$  of the NP powder in dependence on the UV exposure.

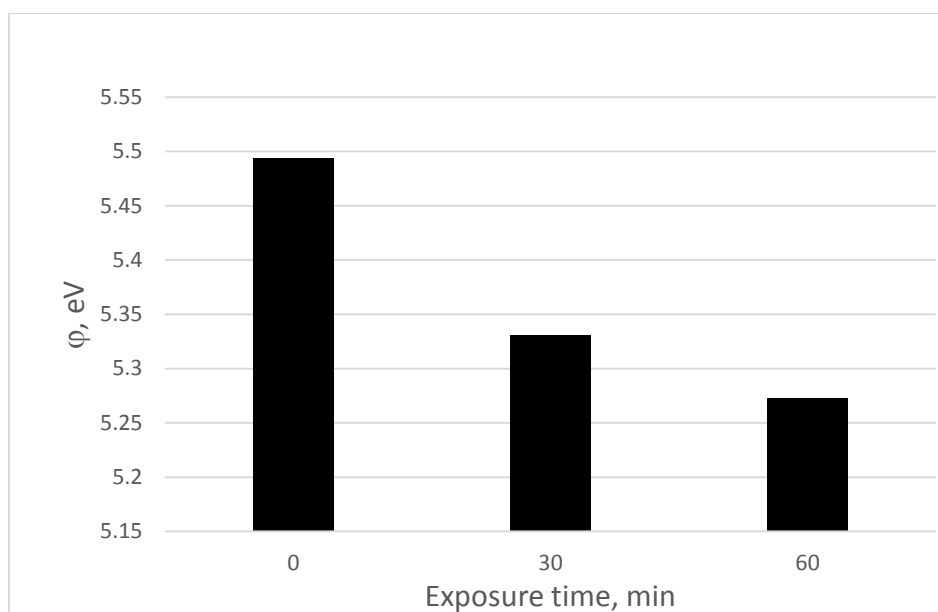


**Figure 1** Influence of the UV exposure on the NP value of  $\phi$  .

The results evidence that UV decreased the barrier for the electron to escape, i.e. the surface became positively charged.

## 2.2. Polymer composite specimens with embedded FNP

The Huntsman epoxy resin *Araldite LY 1564* [7] (at 25 °C: viscosity 1200 – 1400 mPa s, density 1.1 - 1.2 g/cm<sup>3</sup>, epoxy index 5.8 - 6.05 Eq/kg) and the hardener *Aradur 3486* [7] (at 25 °C: viscosity 10 - 20 mPa s, density 0.94 - 0,95 g/cm<sup>3</sup>, Amine value 8.55 - 9.30 Eq/kg) were mixed with the FNP powder. The concentration of the powder was equal to 1.5 % from the resin and hardener total weight (for each specimen - 52.1g of epoxy resin, 17.7g of hardener and 1.75g of nanoparticles)

The mixing was provided at the room condition. The components were mixed during 15 minutes in a dielectric (to avoid leakage of the electrical charge from the FNP) glass stirring rod. To reach the homogeneous composition air bubbles appeared in the mass were evacuated with a vacuum pump (Ozito 12V Air compressor) for 15 minutes. The prepared mixed mass was poured in a tightly closed container from which the air was pumped out at 0.8 bar vacuum.

The fabricated compound was casted in a silicone frame sized to in the square 156.25 cm<sup>2</sup> and having the thickness of 5 mm. The frame was piled on a glass surface greased with TR-104 Hi Temp Mold Release wax (based on the Refined Carnauba Wax blended with synthetic high temperature ingredients and petroleum distillates; dry time 5-10 minutes at 72°F, melt point 180-210°F, penetration hardness 1 at 25°C [8] ). The compound was hardened at the room condition (22°C) during 72 hours. The absence of the air bubbles in the prepared composite plates was verified employing the optical microscopy technique (*Motic BA 400* optical microscope, Meyer Instruments). The specimens were cut off the hardened compound plates in accordance with Figure 2 dimensions. The cutting R0.5 served to get the damage of all of the specimens at an equal location that was necessary because the light beam exciting the PE analyses was

fixed by the optical system (the details are provided below at the paragraph on early destruction identification) and was directed to the damaged area (cutting). To cut off the specimens the milling digitalised machine tool (BLIN, model BL-S360, manufacturer Blin Machinery; milling cutter model BL-S360 having diameter 2 mm and rotation speed 3000 rpm) was employed. After the processing the specimens were washed at the room condition consequently in a distillate water and ethanol for 2 minutes for each wash.

The stretch tests (desctibed below in details) demonstrated that the R0.5 cutting did not influence the shape of the load (F) - elongation (l) diagram, however the values of F and l differed around 10% against the specimens without cutting.

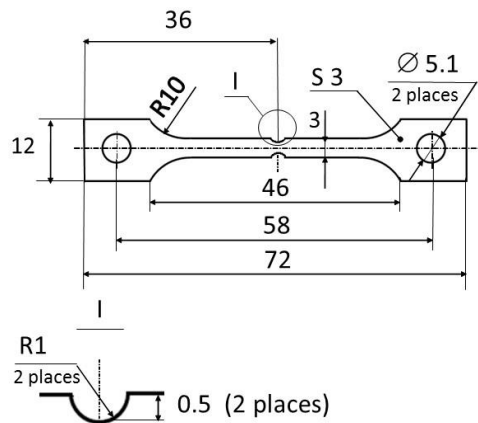


**Figure 2** Dimensions of the specimens (dimensions in mm, tolerance <0.1 mm)

Totally 32 specimens were prepared and tested: 6 specimens per batch had the FNP differently exposed with UV, within the single batch the NP were exposed equally.

### 2.3. Stretch test

The specimens were mechanically tested using the machine IMASH 5C-69 (Russia). Loading was provided with the rate 120 mm/hour in the vacuum condition ( $10^{-2}$  Pa). The elongation (l) and load (F) were measured.

The value of the relative elongation ( $\varepsilon$ ) was estimated as

$$\varepsilon = l/L$$

where  $L=34\text{cm}$  (following the internationally recognised best practice  $L = 11.3\sqrt{S}$ , where  $S$  – area of the native specimen cross section at the destrction/cutting location ( $S=0.06 \text{ cm}^2$ )). The values of F and  $\varepsilon$  at the linear deformation range were in use to estimate the elasticity module E:

$$E = \sigma/\varepsilon$$

$\sigma$  - strain,

$$\sigma = F/S$$

#### 2.4. Identification of early destruction of the specimens

Detection of the PE that appears, when molecular/atomic couples are destroyed because of deformation [9,10] was in use to identify early destruction *in situ* of the specimens loading.

The cutting R2 area (Figure 2) was illuminated (diameter of the light spot was around 5 mm) by UV photons having an energy  $h\nu$  enough to escape the electrons from the specimen and was close to  $\phi$  of the specimens ( $\phi = 5.25 \pm 0.05$  eV it was measured as above) for modulation of the PE current (I) to detect as small as possible variations of  $\phi$  [11] expected because of the molecular/atomic couples reconstruction/destroying and/or development of nano/micro cracks system resulted by deformation.

The UV photons were supplied from the source equal as employed for NP powders radiation. The unfiltered light beam delivered the photons having an energy  $\leq 5.6$  eV [4] that was slightly larger than  $\phi$  to induce I. The latter detected by the secondary electron multiplier VEU6 (Russia) identifying each event of the single electron appearing in the detector (corresponds to the current of  $10^{-19}$  A). The technique was similar as described in [10] and is presented in Figure 3.

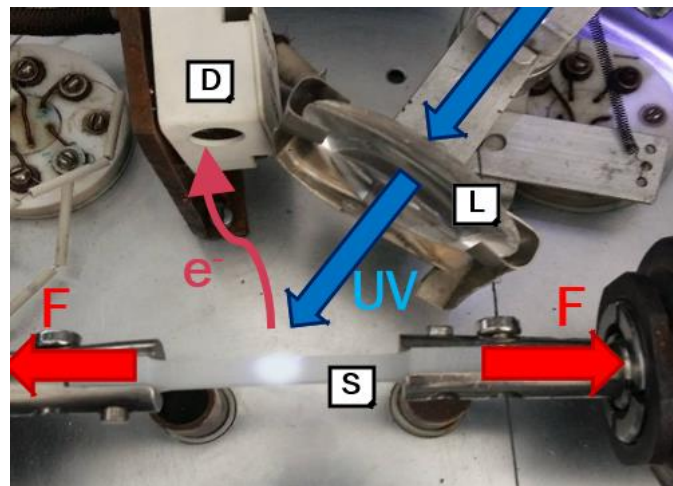


**Figure 3** The vacuum chamber of the equipment for the experiments

F – load, UV- flow of photons, L – quartz lens, D- electron detector, S – specimen,  $e^-$  - electron flow

The electron detector generated impulses that amplitude was amplified and impulses were registered by the radiometer Robotron 20 046 (Germany).

### 3. RESULTS AND DISCUSSIONS

The diagram for  $\sigma$  on  $\varepsilon$  at the elastic range of deformation for the specimens with NP supplied with different UV exposure is shown in Figure 5.

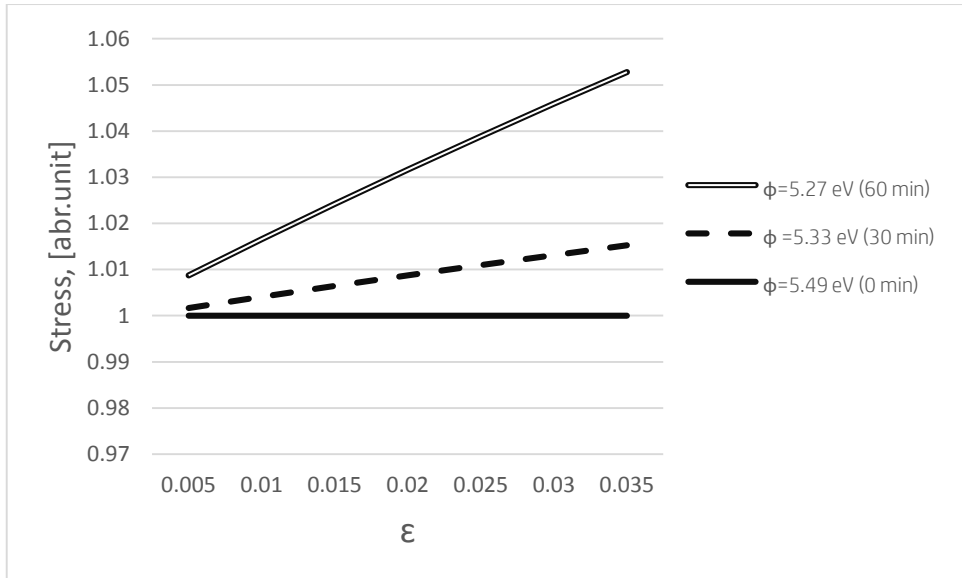


**Figure 4** The strain diagrams at the elastic deformation range of the specimens having NP radiated with different UV exposures.

Following the Figure 4 one could conclude that the positively charged (lower values of  $\phi$ ) NP surfaces increase stress. The ratio of  $\sigma/\epsilon$  (i.e. E) increases, when the FNP acquire higher positive charge.

Figure 5 presents the strength  $\sigma_{st}$  ( $\sigma$  at  $\epsilon \geq 0.035$ ) and E in dependence on  $\phi$  of the FNP.

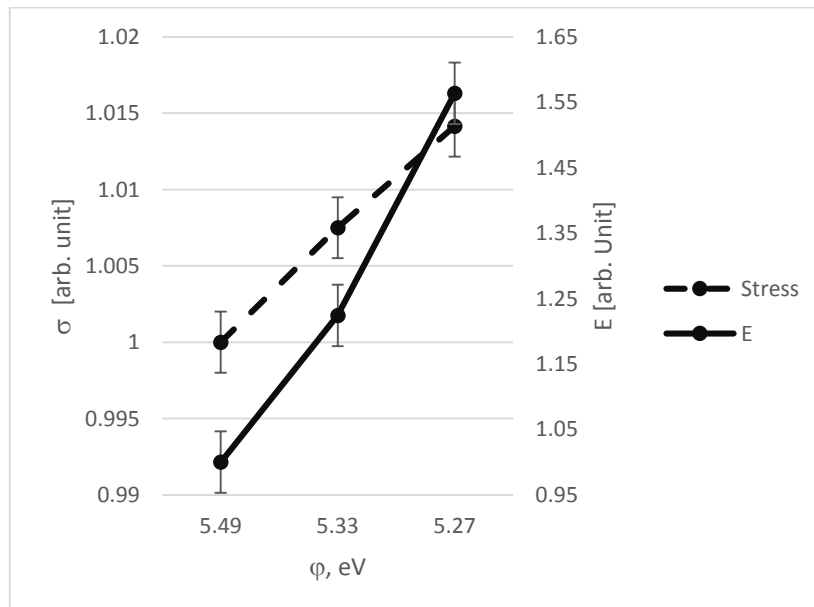


**Figure 5** Correlation of  $\sigma_{st}$  and E with  $\phi$  of FNP embedded in the specimens.

Figure 6 represents typical stress and I diagrams measured in parallel in dependence on duration of deformation/loading.



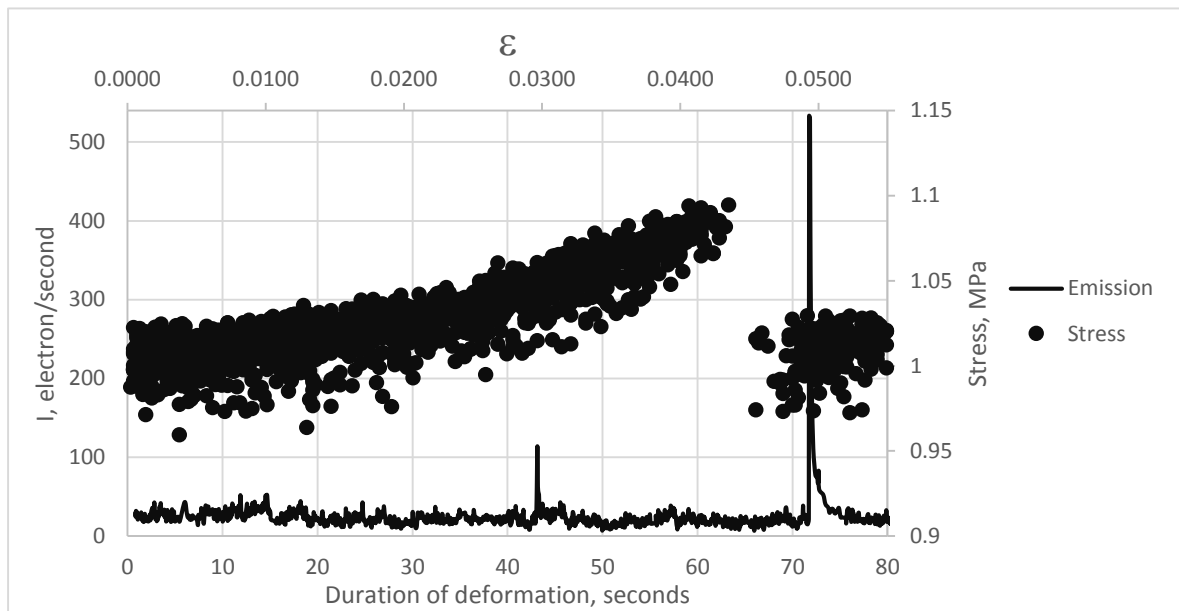


**Figure 6** Typical stress and I diagrams in dependence on deformation duration (NP exposed to 60 minutes of UV) .

The dramatic increase of I was detected at the failure of the specimens. The diagram of I demonstrates the oscillation like behaviour (frequency around 2.7 Hz (Figure 7)) at the area of  $\epsilon$  that raised from 0.01 to 0.04.

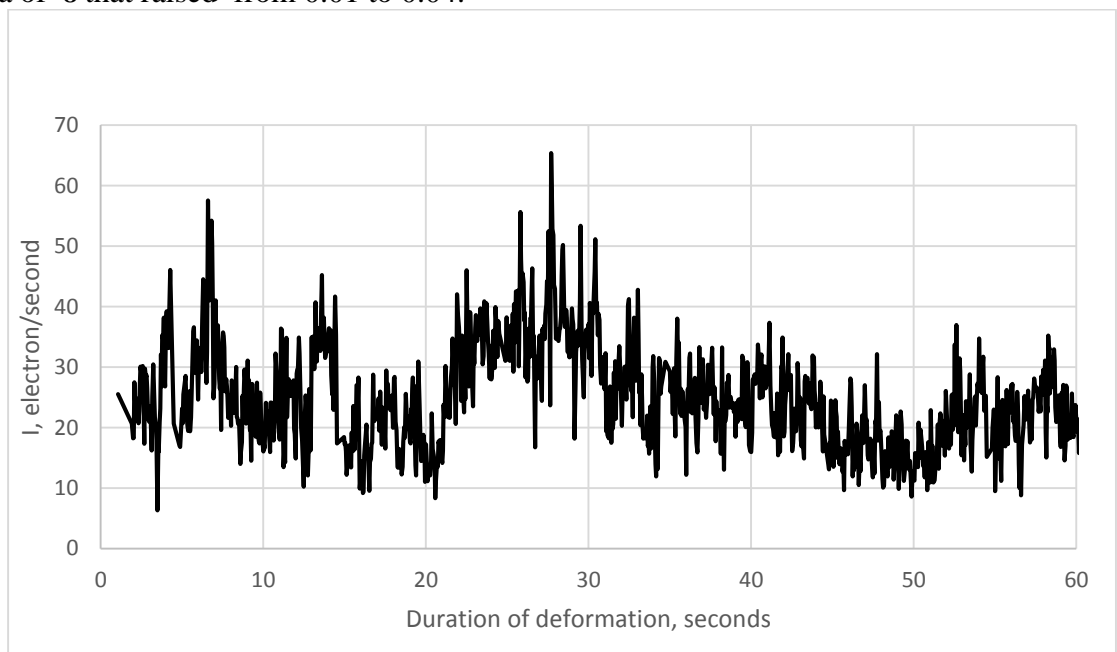


**Figure 7** Oscillation like behaviour of I ( $\epsilon = 0.01 - 0.04$ )

Following [9,10] I behaviour was connected to development of the micro/nano cracks resulted by loading. To identify the start point of  $\epsilon$  for such the supposed phenomenon the I(t) diagrams were treated by the Furrier transform filtering procedure (the OriginPro software was employed). The image of the I(t) signal filtered at the frequency

(f)~ 2.7 Hz with the window  $\Delta f$  that varied in the range from 0.06 to 0.336 Hz demonstrates (Figure 8) the significant antinodes appeared at the very beginning of deformation  $\varepsilon > 0.018$  (arrow).

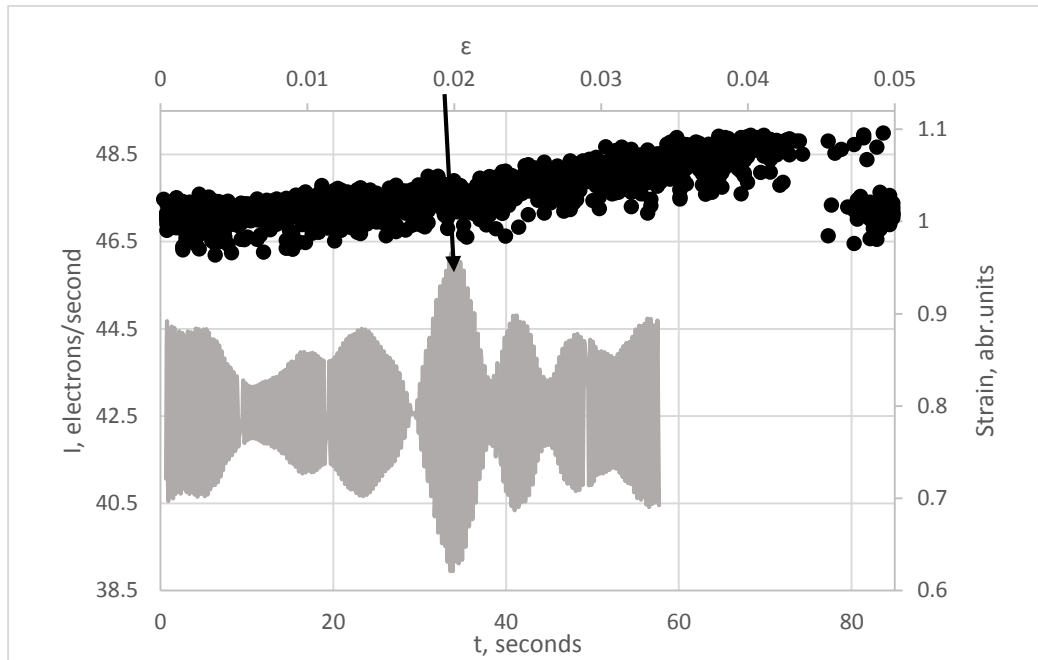


**Figure 8** Typical filtered Furrier image of  $I(t)$  and corresponding stress diagram (specimen having the FNP characterized with  $\varphi=5.29$  eV);  $\Delta f=0.2$  ( $f=2.8$ , Hz).

The values of  $\Delta f$  were varied to detect the antinodes, when they demonstrate their highest relief. Figure 9 provides filtered Furrier images of  $I(t)$  generated with different values of  $\Delta f$  for the specimen having the FNP and characterized with  $\varphi= 5.29$  eV .

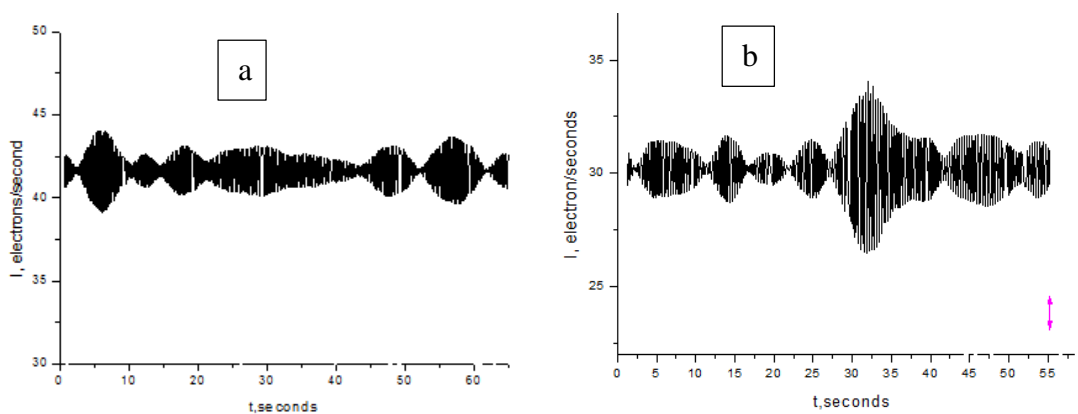


**Figure 9** Filtered Furrier images of  $I(t)$ : a)  $\Delta f =0.4$  Hz , b)  $\Delta f = 0.2$  Hz;  $\varphi= 5.29$  eV.

The value ( $\Delta f_0$ ) of  $\Delta f$  that supplied the highest relief correlates with the magnitude of  $\varphi$  (Figure 10).

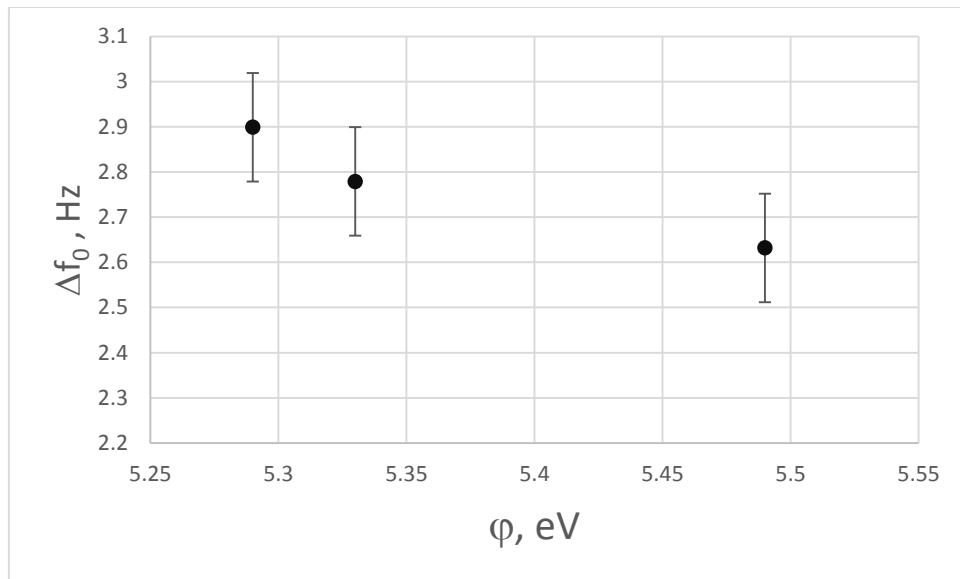


**Figure 10** Correlation of  $\Delta f_0$  with  $\phi$

Such the result is assumed as the signalling of the specimen destruction controlled by differently charged FNP embedded into the prepared PC.

#### 4. CONCLUSIONS

1. The electrically charged SiO<sub>2</sub> FNP embedded into the epoxy resin reinforce it: increasing of the FNP surface positive potential for 0.2 V ( $\phi$  changed from 5.49 to 5.29 to eV) rises strength and elastic module of the composite on ~2% and ~48% correspondingly.
2. Early destruction of epoxy originated composite reinforced with electrically charged SiO<sub>2</sub> FNP starts at the elastic area of deformation beginning at  $\varepsilon \approx 0.018$  (the elastic deformation finished at the value  $\varepsilon = 0.035$ ).
3. Increase of SiO<sub>2</sub> FNP surface electrical positive potential for 0.2 V extends the window  $\Delta f_0$  of the electron emission current frequency related to destruction of the PC. This is assumed as the signalling of the damaging processes that is expected to be analysed in further research.

#### 4. ACKNOWLEDGEMENTS

1. The research leading to the results described in the present article has received the funding from the Latvia State Research Program under the grant agreement "Innovative materials and smart technologies for environmental safety, IMATECH (project Nr 5).
2. The authors are deeply indebted to Mr Igor Kozak for cutting out the specimens and Mr PhD Andrey Aniskevich from the University of Latvia, Institute of Materials Mechanics for sharing the experience of epoxy resin and hardener mixing.

## 5. REFERENCES

1. Q.Yuan, R.D.K. Misra. Polymer nanocomposites: current understanding and issues. *Materials Science and Technology*. 2006, Volume 22, Issue 7, 15. Available from: <http://www.tandfonline.com/doi/abs/10.1179/174328406X101292>
2. Derjaguin B.V., Landau L.D. *Acta Physic Chimica*, USSR, **14**, 633-642, (1941).
3. A-M El-Sayed, K Tanimura, A L Shluger. Optical signatures of intrinsic electron localization in amorphous SiO<sub>2</sub> *J. Phys.: Condens. Matter* 27 (2015) 265501 (6pp) doi:10.1088/0953-8984/27/26/265501
4. Hamamatsu Lightningcare LC5 data sheet. Available: [http://www.helmutsinger.de/pdf/hamamatsulc5\\_lc6.pdf](http://www.helmutsinger.de/pdf/hamamatsulc5_lc6.pdf)
5. Carlson T.A., "Photoelectron and Auger Spectroscopy". Plenum Press, 1975, 417 pages
6. M. Zakaria, Y. Dekhtyar, T. Bogucharska, V. Noskov. Exoemission Instrument and Technology to Explore Gamma Radiation Influence on Bones. *dPhysica Medicaan Inf Medicaunce on Bo*,47-49
7. HUNTSMAN, Advanced materials: Araldite® LY 1564\* / Aradur® 3486\* / Aradur® 3487. 2012. Available: <https://www.swiss-composite.ch/pdf/t-Araldite-LY1564-Aradur3486-3487-e.pdf>
8. T.R. Industries, TR-104 Hi-Temt Mold release wax, 2013. Available: [http://www.compositesone.com/wp-content/uploads/2013/07/TR-104\\_TDSeng.pdf](http://www.compositesone.com/wp-content/uploads/2013/07/TR-104_TDSeng.pdf)
9. W. J. Baxter, S. R. Rouze Photostimulated exoelectron emission from slip lines: A new microscopy of metal deformation. *Journal of Applied Physics* 44, 4400 (1973); doi: 10.1063/1.1661972.
10. Yu. Dekhtyar, Y. Kawaguchi, A. Arnautov. Failure and relaxations of carbonbre-reinforced plastic tested by exoemission and luminescence methods. *Int. J. Adhesion and Adhesives* 17 (1997) 75-78
11. Yu. D. Dekhtyar, Yu. A. Vinyarskaya Exoelectron analysis of amorphous silicon. *J. Appl.P hys.* 7 5 (8),1994, 4201-4207. N. B. Kinding, W. E. Spicer ,*Phys .Rev A* 138,561( 1963) .